Int J Adv Manuf Technol
DOI 10.1007/s00170-010-2678-3

ORIGINAL ARTICLE

Torque control of friction stir welding for manufacturing and automation

William R. Longhurst · Alvin M. Strauss · George E. Cook · Paul A. Fleming

Received: 17 June 2009 / Accepted: 13 April 2010

Abstract Friction stir welding (FSW) is a solid-state welding process that utilizes a rotating tool to plastically deform and forge together the parent materials of a workpiece. The process involves plunging the rotating tool that consists of a shoulder and a pin into the workpiece and then traversing it along the intended weld seam. The welding process requires a large axial force to be maintained on the tool. Axial force control has been used in robotic FSW processes to compensate for the compliant nature of robots. Without force control, welding flaws would continuously emerge as the robot repositioned its linkages to traverse the tool along the intended weld seam. Insufficient plunge depth would result and cause the welding flaws as the robot's linkages yielded from the resulting force in the welding environment. The research present in this paper investigates the use of torque instead of force to control the FSW process. To perform this research, a torque controller was implemented on a retrofitted Milwaukee Model K milling machine. The closed loop proportional, integral plus derivative control architecture was tuned using the Ziegler–Nichols method. Welding experiments were conducted by butt welding 0.25 in. (6.35 mm)×1.5 in. (38.1 mm)×8 in. (203.2 mm) samples of aluminum 6061 with a 0.25 in. (6.35 mm) threaded tool. The results indicate that controlling torque produces an acceptable weld process that adapts to the changing surface conditions of the workpiece. For this experiment, the torque was able to be controlled with standard deviation of 0.231 N-m. In addition, the torque controller was able to adjust the tool's plunge depth in reaction to 1 mm step and ramp disturbances in the workpiece's surface. It is shown that torque control is equivalent to weld power control and causes a uniform amount of energy per unit length to be deposited along the weld seam. It is concluded that the feedback signal of torque provides a better indicator of tool depth into the workpiece than axial force. Torque is more sensitive to tool depth than axial force. Thus, it is concluded that torque control is better suited for keeping a friction stir welding tool properly engaged with the workpiece for application to robotics, automation, and manufacturing.

Keywords Friction stir welding · Torque control · Force control · Robotic friction stir welding · Automation · Manufacturing

Nomenclature

F_t	traverse force (Newton)
K_p	proportional gain
K_i	integral gain
K_d	derivative gain
M	torque (Newton-meter)
R	radius of the shoulder (meter)
e	force error (Newton)
mm	millimeters
r	radius of the pin (meter)
s	complex variable
t	pin length (meter)
$\underline{t}$	time (seconds)
u	control signal
v	traverse velocity (millimeter/s)
π	pi
σ	shear flow stress (Newton/m^2)
ω	angular rotation velocity (radians/s)

W. R. Longhurst (✉) · A. M. Strauss · G. E. Cook · P. A. Fleming
Welding Automation Laboratory, Vanderbilt University,
Featheringill Hall Rm. 118,
Nashville, TN 37235, USA
e-mail: russ.longhurst@vanderbilt.edu

Published online: 28 April 2010

1 Introduction

Friction stir welding (FSW) is a material joining process that was invented by Wayne Thomas of The Welding Institute and patented in 1995 [1]. During the joining process, the parent materials remain in their solid state unlike fusion welding processes that require the parent materials to be melted. Because the parent materials remain in the solid state, FSW offers many advantages over fusion welding processes. These advantages include reduced porosity, increased mechanical strength, and no filler material or welding fumes. Primarily, FSW is used to join metals with low melting points such as aluminum and copper.

The FSW process utilizes a rotating nonconsumable tool to perform the welding process. In its simplest form, the rotating tool consists of a small pin (or probe) underneath a larger shoulder. Metal flow caused by the tool is very complex and is an area where a great deal of research is ongoing. One accepted model that provides insight into the metal flow phenomena and the resulting joining of the parent metals is the Arbegast model [2]. Arbegast's model of metal flow describes five zones within the welding process. The five zones are: preheat, initial deformation, extrusion, forging, and lastly, the cool down. The preheating of the metal occurs due to the transfer of heat ahead of the traversing tool. The initial deformation occurs as the soften metal ahead of the tool begins to deform due to the rotation of the tool. Next, as the tool advances into the heated and slightly deformed metal, the rotating pin extrudes the metal around to the backside of the pin where it is subjected to high forging pressure from the shoulder. Once the metal has been extruded to the backside of the pin and forged together, it has undergone serve deformation but has remained in its solid state. As the newly forged metal exits from underneath the backside of the shoulder, it begins to cool either naturally or through some forced convection method. Figure 1 illustrates the FSW process as described by Arbegast's model.

Historically there have been three process parameters used to control FSW during steady-state conditions. They are the FSW tool's plunge depth, rotation rate, and traverse rate. However, as FSW evolved from its infancy, the axial force placed on the workpiece by the tool became a very important process parameter. The reason for its emergence as an importance parameter is linked to the application of FSW with robots. Similar to other welding technologies, the application of FSW with robots provides a very flexible platform for automation. However, with FSW the relatively large forces present a challenge. The load bearing capability of robots is limited and thus most robots are not well suited for FSW. In addition, their compliant nature makes FSW much more challenging.

To address the compliance problem, force control has been presented as a solution. With robotic FSW the challenge is to keep the tool positioned correctly with adequate force on the tool, while the linkages of the robot continually reposition themselves. The motion of the linkages, along with their reaction to the large welding forces, results in positioning errors of the tool. In conjunction with these positioning errors, large fluctuations in the forging force results within the welding environment. These positioning errors and force fluctuations will possibly lead to insufficient deformation, forging, and consolidation of the parent metals. With force control, constant axial force is maintained on the tool and the likelihood of welding flaws is diminished.

Successful applications of robotic FSW have been documented with work by Smith [3], Soron and Kalaykov [4], and Zhao et al. [5]. Each of these groups developed and implemented a force control architecture using plunge depth as the controlling variable. All were able to conclude that it was feasible to implement FSW force control architectures. However, force control of FSW remains difficult and its operation confined to a limited range of process parameters due to the highly nonlinear welding environment. Smith used a force control architecture based upon a Jacobian relationship between motor torques and

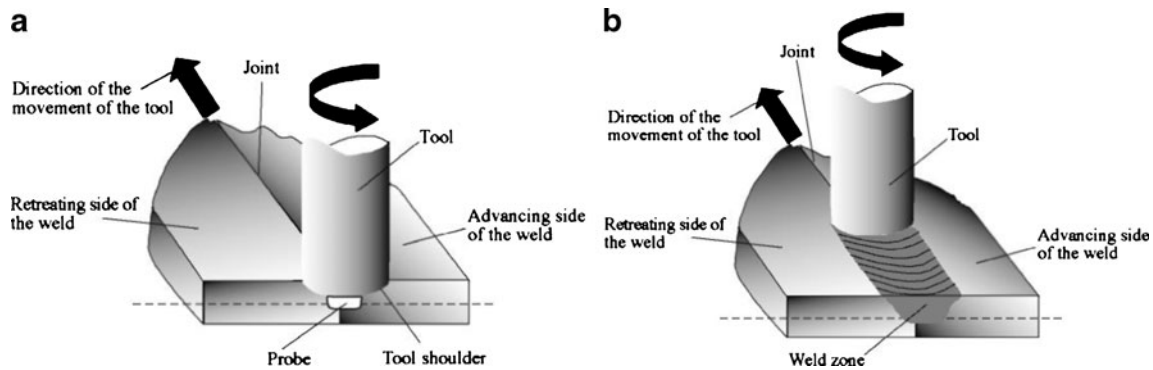

Fig. 1 FSW process [10]

welding forces [6]. He was successful but the controller was stable for a limited range of process parameters and a controller update frequency of less than 2 Hz. Soron and Kalaykov concluded that even with the added force control to the robotic FSW system, axial force oscillations still exist when the tool makes contact with the material. They also note the penetration depth is hard to predict due to the positioning error of the robot. Zhao et al. presented a nonlinear axial force controller they developed and implemented for a FSW process. They were able to experimentally model the static and dynamic behavior of the interaction between the FSW tool and the workpiece. With this information and using an open architecture control system, they were able to design a controller using polynomial pole placement. Good results were obtained, but to handle the nonlinear transient response when the tool's plunge depth changed, the control system had to incorporate experimentally obtained dynamic parameters. Thus, the controller's parameters were specific to their experimental setup.

Even with these advances, the problems associated with robotic FSW are not solved. As noted by Soron and Kalaykov, problems still exist with force oscillations. The highly nonlinear aspect of the welding environment makes it extremely difficult to implement a robust system that maintains stability over a large range of process configurations and parameters.

Research by Fleming [7] introduces the potential for torque as a feedback signal for seam tracking of FSW lap weld joints. His work on other tracking algorithms had used axial force as the feedback but a high amount of noise in the force signal caused him to explore torque as the feedback signal. Could a similar situation be present with force control of FSW?

The research presented in this paper introduces and examines torque as a controlled parameter instead of axial force. A torque control architecture that varies plunge depth to maintain a desired torque is implemented on a three-axis milling machine. The resulting performance of the torque controller is analyzed and relationships between axial force and torque are defined. Features are identified that make torque control more attractive than force control. It is concluded that controlling the torque provides a better indication of plunge depth than force.

2 Experimental setup

The experiment was conducted on the FSW system at Vanderbilt University which is shown in Fig. 2. The FSW system is a Milwaukee Model K milling machine that has been retrofitted with more advanced motors and instrumentation. These retrofits were previously added to automate the system and provide a programmable platform for FSW experimentation. At the top of the control hierarchy is a master computer that enables all of the systems subcomponents such as the motor drive controllers and instrumentation. The master computer is a Dell Precision 340 that uses Microsoft Windows XP as its operating system. The welding and torque control code was written in C#. A graphical user interface within the C# software allows the operator to select the desired welding parameters for the pending operation. These parameters include the FSW tool's rotation speed, traverse speed, plunge depth, and weld path position.

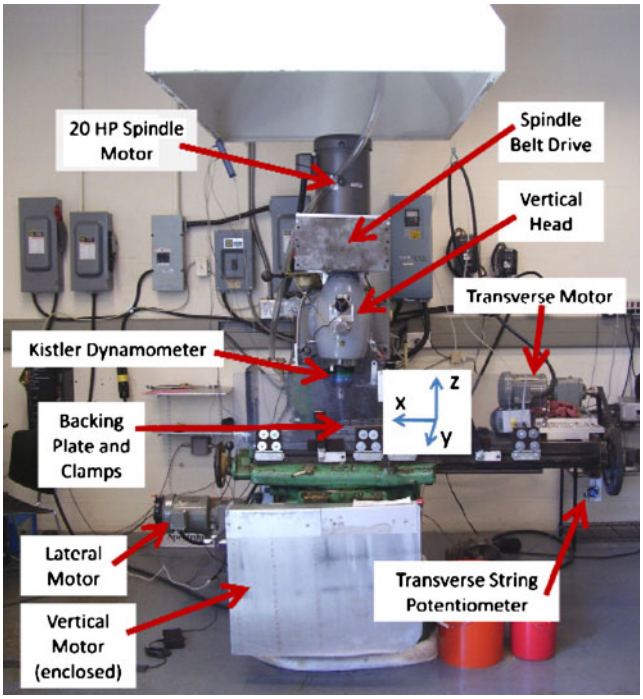

Fig. 2 FSW machine at Vanderbilt University

The tool's z-axis coincides with the milling machine worktable's vertical axis when the tool is at a zero degree tilt angle. The worktable resides on the knee that is mounted to a vertical positioning screw and secured in sliding dovetail joints. The knee travels on the screw via a gear system inside the knee. An externally mounted belt and pulley system is attached to the input shaft of the gear system. Power is provided by a Parker Compumoter KH series brushless servo motor. The servo motor is controlled by a Parker Compumotor KHX-250 servo drive that utilizes a proportional, integral plus derivative (PID) control algorithm. Command signals are sent directly from the master computer to the servo drive. Vertical position of the table is obtained from a Renishaw linear scale that has a resolution of 10 μm. Position data from the sensor is fed into a sensor box where it is converted to a digital signal prior to being sent to the master computer.

Welding force data is collected through a Kistler rotating cutting force dynamometer. The dynamometer collects *x*-axis force, *y*-axis force, and *z*-axis force as well as the torque about the *z*-axis. The analog signal from the dynamometer is sent to a signal conditioning box where it is converted from an analog signal to a digital signal. Once converted the data is sent to a separate computer where the data is sorted, recorded, and displayed before being sent to the master computer.

An overview of the closed loop torque control system is illustrated in the control block diagram of Fig. 3. Within the master computer, a desired torque is selected. The desired torque value is subtracted from the actual torque value to obtain a torque error. The torque error signal is then processed in the control law. The servo drive produces a change in the vertical position of the tool which results in a change of the torque acting on the tool. The dynamometer reads the resulting torque and returns it to the master computer where it is once again compared to the reference signal.

The servo motor operates in a continuous mode and turns the output shaft based upon the value of the processed error signal. For this mode of operation, velocity and acceleration profiles were preprogrammed for complete motion control of the output shaft and the movement of the FSW tool. For the experimental setup a motion profile was chosen that resulted in the system having smooth acceleration and deceleration. This increased the stability of the torque controller by reducing the magnitude of the transient torque response of the system. A trapezoidal velocity profile was chosen and preprogrammed into the torque controller. With the trapezoidal profile, the acceleration was always constant at the beginning and end of the motion. The torque controller would determine the amount of the torque error, process the error signal according to the control law, and send a motion command to the servo drive. The preprogrammed motion profile was scaled by the torque controller to the size of the processed error signal before being sent to the servo drive.

The measured torque signal was very noisy. This noise makes the process of applying derivative control to the system very difficult. The noise would simply be amplified by the controller. To address this problem, a filter was implemented. The filter is a five-point moving average of the torque with an interrupt frequency of 3.33 Hz. For this experimental setup, these filter parameters were found to provide adequate noise reduction without adding too much phase lag in the signal.

To create and investigate the performance of torque control via plunge depth, a PID control architecture was chosen. To tune the PID torque controller and achieve optimum control, the Ziegler–Nichols tuning method was used [8]. The Ziegler–Nichols tuning method called for the controller to use only proportional control while welding. While using proportion control only, a critical gain value was experimentally determined through trial and error. Over the course of several welds, the gain was steadily increased until the resulting torque achieved sustained oscillation. The sustained oscillation constituted marginally stable behavior. The resulting control gain and time period between oscillations was recorded and used to calculate PID gains for the controller. The resulting PID control law is shown in Eq. 1. In Eq. 1, K_p is the proportional gain, K_i is the integral gain, K_d is the derivative gain, e is the error, and u is the resulting control signal as a function of time t.

$$K_p e + K_i \int e + K_d e' = u(t) \tag{1}$$

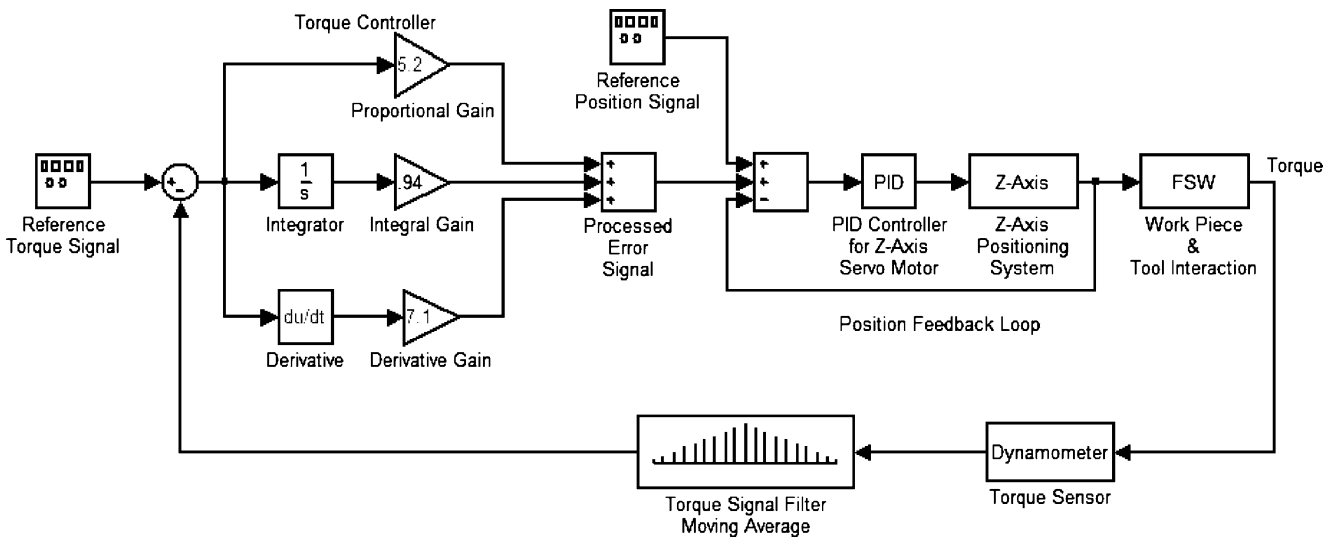

Fig. 3 Block diagram of torque control via plunge depth

For this torque control research, a 0.25 in. (6.35 mm) treaded tool was selected. A picture of the tool is shown in Fig. 4. The threaded pin was 0.235 in. (5.969 mm) long with a diameter of 0.250 in. (6.35 mm) across its threads. The shoulder was of a hybrid nature. It had a flat 0.625 in. (15.875 mm) diameter shoulder that acted as the forging surface. The remaining portion of the shoulder was on a 7° taper that started at the 0.625 in. (15.875 mm) diameter point and continued to the 1 in. (25.4 mm) outermost diameter. The tool was positioned on a 1° lead angle relative to the workpiece. From the Ziegler–Nichols tuning method, the critical gain and period for the 0.25 in. threaded tool was 8.6 and 11.0 s. The resulting control gains are shown in Table 1.

For the experiment 0.25 in. (6.35 mm) butt welding with full penetration was performed. The material used was aluminum 6061. The workpiece consisted of two 0.25 in. (6.35 mm) by 1.5 in. (38.1 mm) by 8 in. (203.2 mm) long samples. Each weld began with the tool plunging into the metal 1 in. (25.4 mm) from the end of the workpiece. Once the tool achieved the desired plunge depth, it dwelled at that location for 5 s in order to soften the workpiece by generating additional heat. After dwelling, the tool began to traverse forward at either 6 $\mathrm{in.min^{-1}}$ (IPM) (152.4 mm $\mathrm{min^{-1}}$) or 3 IPM (76.2 mm $\mathrm{min^{-1}}$). After traversing 1 in. (25.4 mm), the torque controller was engaged. The torque controller was operating in a regulation mode, meaning whatever the torque was at the time of engagement, was the selected desired torque. The system operated under torque control mode until it reached 1 in. (25.4 mm) from the end of the 8 in. (203.2 mm) workpiece. Thus, 5 in. (127 mm) of welding was conducted each time under torque control. For every weld made, the tool's shoulder was initially plunged between 0.000 and 0.002 in. (0.000–0.051 mm) below the surface and the tool's rotation rate was maintained at a constant 1,400 revolutions per minute.

Fig. 4 FSW tool used for torque control

Table 1 Torque control gains

Threaded Tool Torque Control (0.25in.)			
	K_p	K_i	K_d
PID	5.16	0.938	7.095
P	4.3		
PI	3.87	0.422	
PD	3.87		3.192

K_α=8.6, P_α=11

3 Results and discussion

The resulting torque can be seen in the data of Fig. 5. As the tool slowly plunged into the workpiece, the torque steadily increased. The plunge began at approximately 120 s and ended at 220 s. At the end of the plunge, the tool dwelled for 5 s. While the tool was dwelling, the torque slowly decreased about 2.5 N-m. Once the dwelling was complete, the tool began traversing forward. As the tool began to move forward, a relatively large spike in torque occurred. However, the torque returned to its original value after about 5–7 s. The most probable cause of this transient response was the built-up ridge of material surrounding the tool from its initial plunge into the workpiece. The tool must travel through this ridge during the first few seconds of forward movement.

After 1 in. (25.4 mm) of forward travel, the torque control is engaged. The torque control engagement is noted by the desired torque curve in Fig. 5. As can be seen in Fig. 5, the torque is regulated to the desired value. This torque is maintained until the end of the weld. At the end, the tool is retracted from the workpiece.

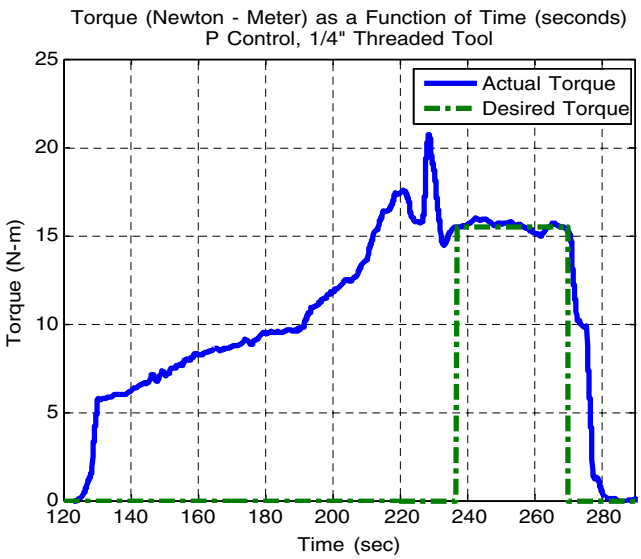

Fig. 5 Torque controlled response

The results of Fig. 6 provide more detail into the performance of the torque controller. A close-up view of the torque curve during torque control is present. Statistical analysis reveals the controller was able to obtain a mean torque of 15.57 N-m with a standard deviation of 0.231 N-m. The desired torque the controller was trying to obtain was 15.52 N-m. The range of torque was 1 N-m with a maximum value of 15.98 N-m and a minimum value of 14.98 N-m. The median value was 15.6 N-m.

To control the torque, the plunge depth had to be adjusted over a range of approximately 0.005 in. (0.127 mm). The position of the worktable is shown below the torque data in Fig. 6. The first adjustment was the retracting of the tool to reduce the plunge depth. As the tool approached the end of the workpiece, the torque had to be increased two separated times by plunging the tool deeper into the workpiece. Since the workpiece was flat, the adjustments can be attributed to the changing thermal conditions within the workpiece and not physical changes in the workpiece's surface. The first adjustment occurred to reduce the torque as the tool was moving into a colder weld region. The last two adjustments were needed to increase the torque because the welding environment had grown softer due to the build up of heat near the end of the workpiece.

Using axial force control instead of torque control produces similar results. It is difficult to compare the two methods statistically since the outputs have different units, but qualitatively they can be compared. The most notable similarity is the amount of adjustment in plunge depth needed. Force control experiments conducted with this same FSW equipment required a range of 0.005 in. (0.127 mm) in adjustment to maintain a desired force. As evident from the data in Fig. 6, this proved to be the same case with torque control. The same can be said about the adjustment to the step disturbance. Both force and torque control required the same amount of plunge depth adjustment to 1 mm step disturbances.

When the FSW system is operating under torque control, a constant amount of power is input into the welding environment. In a sense, energy control emerges as a by-product of torque control. This is evident by the results shown in Fig. 7. In Fig. 7, the input power (Watts) and the energy per unit length of weld (Joules per millimeter) is defined by Eqs. 2 and 3. In these equations, P is the power, F_t is the traverse force, v_t is the traverse velocity, M is the torque, and ω is the tool rotation speed.

$$P = (F_t \times v_t) + (M \times \omega) \quad [\text{Watts}] \tag{2}$$

$$E = P/v_t \quad [\text{Joules/mm}] \tag{3}$$

With welds made at low speed, a large majority of the input power is due to the torque and rotation speed. When constant torque is maintained by the controller, the input power and energy per unit length of weld is approximately constant as well. The small variation is attributed to the small variation of the torque and the traverse force.

The torque controller's response to physical changes on the workpiece surface is shown in Figs. 8–11. Figure 8 shows the response to a 1-mm step change in thickness of the workpiece. The welded sample with the 1 mm step can be viewed in Fig. 9.

As the tool traversed across the surface, it encountered the torque disturbance. To reject the disturbance and return the torque back to its desired value, the worktable had to move downward 1 mm. As can be seen in Fig. 8, the controller successfully accomplished this. It took the

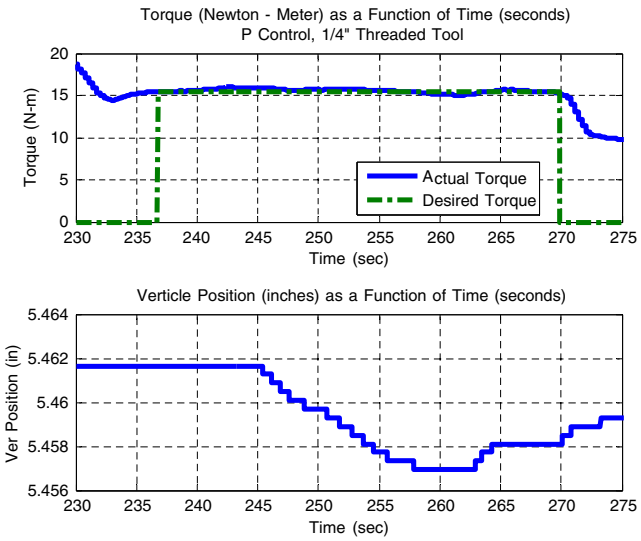

Fig. 6 Regulation of the torque

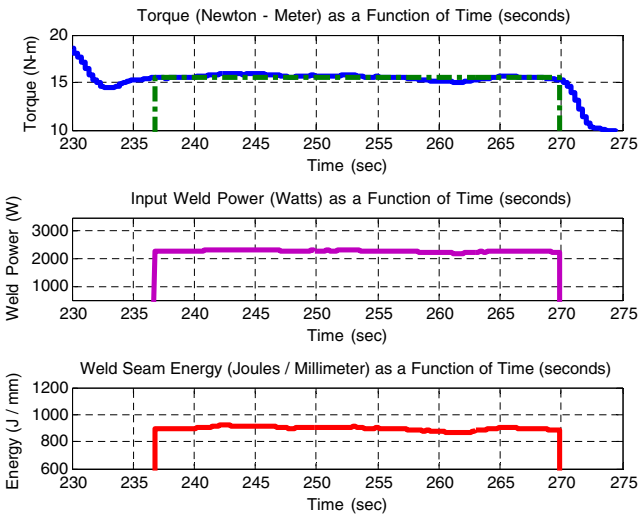

Fig. 7 Energy model of FSW while under torque control

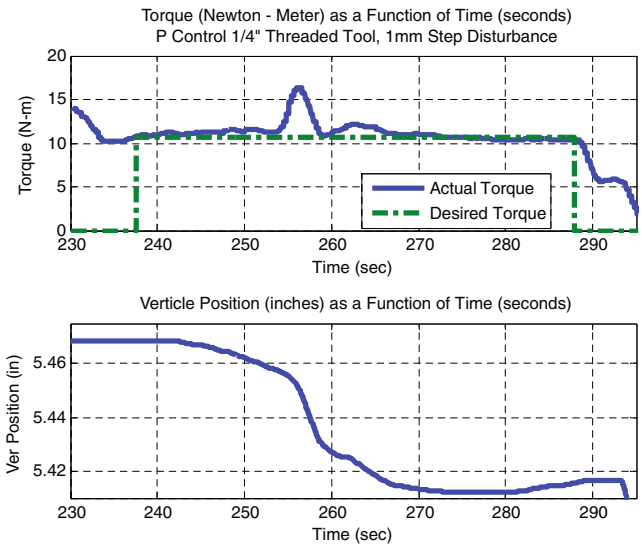

Fig. 8 Step disturbance (1 mm)

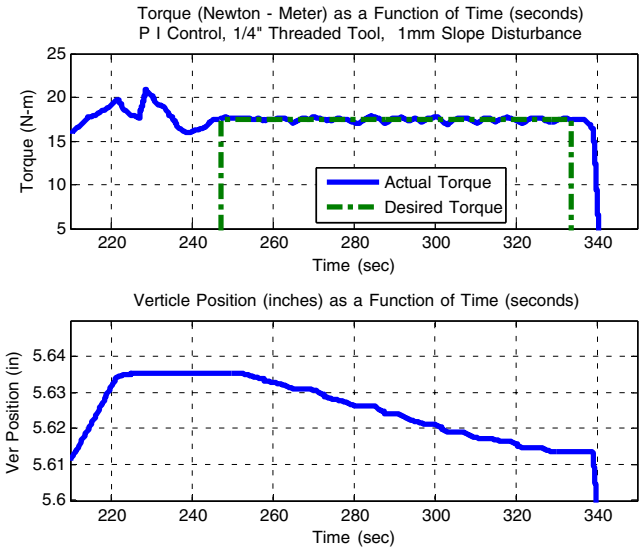

Fig. 10 Ramp disturbance (1 mm)

controller approximately 25 s to adjust to the change in the workpiece's surface.

The response to a ramp disturbance is shown in Figs. 10 and 11. To create the disturbance, the workpiece was placed on an incline. The incline resulted in one end of the workpiece being 1 mm higher than the other. The resulting force and worktable position are shown in Fig. 10. The controller adjusted the tool's position quite well and maintained a nearly constant torque over the course of the weld.

Figure 11 is a picture of the welded workpiece that was position on an incline. The resulting weld is void of excess weld flash, thus indicating the controller was able to adjust the tool to the continuously changing workpiece's surface. Without torque control, this would not be possible. To illustrate the difference, a weld was made with the workpiece on the identical incline, but without the use of torque control. The results are shown in Fig. 12. As can be seen, an excessive amount of flash was generated due to the tool digging into the material and not adjusting to the changing workpiece's surface.

To investigate the relationship between axial force and torque, the torque data in Fig. 5 is shown again in Fig. 13, but with the corresponding axial force. During the region of control, the force follows the same trend as the torque. When the torque decreases, so does the force. Likewise when the torque is increased, the force increases. However, there is a very distinct difference in torque and force during the initial plunge of the material.

Notice in Fig. 13 how the torque steadily increases as the tool is plunged into the workpiece. This is occurring between the times of 120 to 220 s. In contrast, the force is not steadily increasing. The force curve has three distinct regions. The regions are the initial rise in force due to the pin contacting the workpiece, the reduction in force as the pin continues to plunge, and the increase in force due to the shoulder contacting the workpiece. What is interesting about this comparison is the fact that torque is more representative of the actual plunge depth.

To understand why torque is more closely related to the plunge depth, let us look at the mathematical definition of torque as given by Nunes et al. [9]. Nunes et al. use a rotating plug model to develop the equation for torque. He theorizes a small volume of material sticks and rotates with the tool. According to Nunes, shearing of the workpiece occurs at a shear interface boundary and not at the tool's

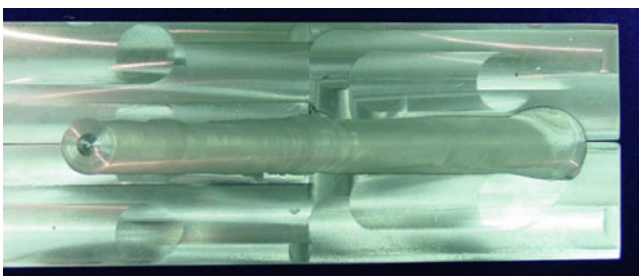

Fig. 9 Weld sample with 1 mm step

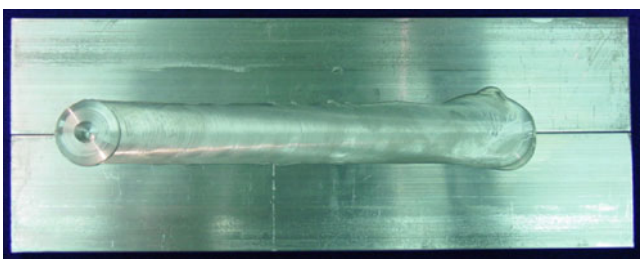

Fig. 11 Weld sample with 1 mm ramp

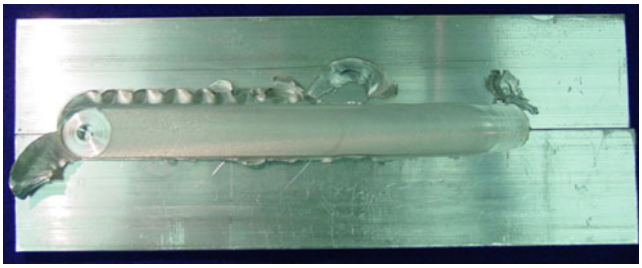

Fig. 12 Weld sample with 1 mm ramp and no torque control

surface. The pressure needed for shearing and subsequent deformation at the interface boundary is simply the shear flow stress σ. Approximating the surface of the shear interface boundary as the surface of the tool, the torque M can be computed with Eq. 4.

$$M = \text{Torque on Shoulder} + \text{Torque on Pin Sides} + \text{Torque on Pin Bottom} = \int_r^R 2\pi r\sigma \mathrm{d}r + 2\pi r^2 t\sigma + \int_o^r 2\pi r^2 \sigma \mathrm{d}r \quad (4)$$

In Eq. 4, R is the radius of the shoulder, r is the radius of the pin, t is the length of the pin, and σ is the shear flow stress. The resulting torque in Fig. 13 can be explained by using Eq. 4. At the moment of contact between the bottom of the pin and the workpiece, the torque quickly rises. The torque at this point is only acting on the bottom of the pin. Thus, the third part of Eq. 4 is used to determine the torque. Since the bottom of the pin is flat, it only takes a few seconds for the bottom of the pin to be submerged below the surface and hence, the sharp increase in torque at the beginning of the plunge. The steady increase in torque is attributed to the second portion of Eq. 4. The second portion of the equation defines the torque along the sides of the pin. Its value is directly proportional to the depth of the pin into the workpiece. Thus, this can explain the steady and rather linear increase in torque as the tool is plunged further into the workpiece. At the end of the plunge, there is a noticeable increase in torque. This is due to the shoulder contacting the workpiece. Mathematically, it can be explained with the addition of the first portion to the overall value of the torque.

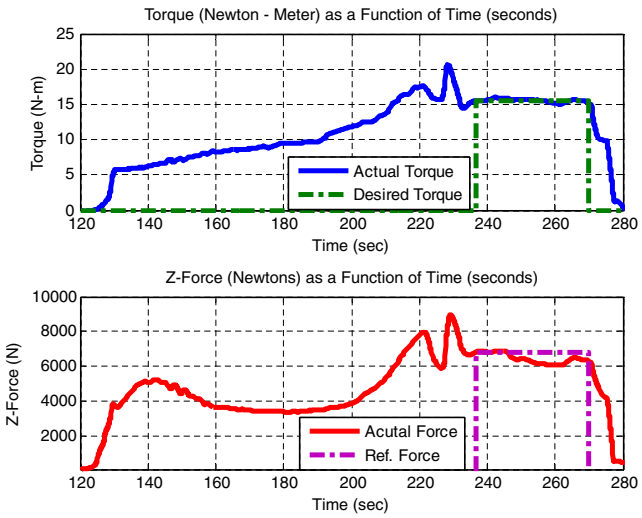

Fig. 13 Recorded torque and force during welding

Torque is also a function of the shear flow stress of the workpiece. The shear flow stress is temperature dependent, thus as more heat is generated and the workpiece becomes softer, the shear flow stress reduces. However upon comparison, torque appears to be less sensitive to thermal conditions than does force. In addition, a change in axial force is dependent upon a change in the amount of tool surface area in contact with the workpiece. For instance, as the pin continues its path downward into the material during the initial plunge, there is no further change in tool surface area perpendicular to the axial direction. Once the bottom of the pin is submerged, no further changes occur until the shoulder reaches the surface of the workpiece. With no change in surface, there is no increase in force. The additional heat added during the plunge reduces the force as the pin is plunged. Thus, using force to predict tool depth is not advised. However, using torque to predict tool depth does have potential.

Lastly, in the absence of a commercial force sensor such as a dynamometer, torque can be easily measured with strain gauges attached to the tool. Measuring the elastic twisting of the tool is much more viable than trying to measure the axial deformation. The axial deformation will be greatly affected by thermal expansion whereas deflection due to torsion will not be as sensitive to an elevated temperature. As another possibility, the torque acting on the tool could be obtained by measuring the current used to power the spindle motor.

4 Conclusions

From the results, it is concluded that using torque control is an attractive alternative to force control. It is attractive because of its sensitivity to tool depth into the workpiece. When articulated arm robots are used for FSW, the control algorithm must accommodate for deflection and positioning errors of the robot. In the past, force control has been used to accomplish this task. However, due to the highly nonlinear relationship between axial force, and the process parameters of plunge depth, rotation speed, and traverse speed, the use of force control is restricted to a range of processing parameters.

Torque control has the potential to increase the range of processing variables suitable for stable control. Preliminary results from other experimentation at Vanderbilt University support the conclusion that torque control is more attrac-

tive. FSW of pipe and pressure vessel sections using a rotary positioning device in place of the traverse axis was setup on the same FSW system described earlier. Using force control to adjust to the concentricity of the parts and the deflection of the rotary device, circular seam welds were produced. However, this rotary setup created abnormally hot welding conditions. With the circular configuration of the parts, the heat was trapped in the workpiece and could not conduct away from the workpiece. As the heat continued to build within the workpiece, the stiffness of the welding environment changed drastically over the course of the seam weld. Near the end of the weld, force control was not working effectively. The tool would tend to dig into the material with no relative change in force realized. However when torque control was used, a more desired response occurred. The tool was better able to track the surface of the workpiece as it rotated one complete revolution.

Torque control also provides a method to control the weld power. Since weld power is predominately a function of torque and tool rotation speed, the input power remains constant under torque control. Along with constant input power, a uniform amount of energy per unit length of weld is deposited into the weld seam.

Future work could attempt to quantify the range of process variables for stable torque control. In addition, work could be performed to see which tool geometries work best with torque control. A flat shoulder creates a more sensitive region where a very small change in plunge depth will produce a relatively large change in torque. An increased lead angle could create more stable control systems by eliminating the large and relatively instantaneous change in torque associated with a flat shoulder.

More importantly, work can be done to develop a measurable correlation between tool depth and torque. There would be great potential for use of torque as a feedback signal indicating tool depth. Until a measurable correlation can be established, the combined use of force and torque control should be exploited for maximum robustness of robotic FSW systems. A possible course of direction would be to control torque as cited in this paper while monitoring the force. If the axial force exceeded pre-established limits, a process alarm could be generated indicating the possibility of a welding flaw. Both axial force and torque are important regarding the production of quality welds, but torque would be better suited as the primary parameter to control due to its sensitivity of tool depth. Controlling torque has great potential for the advancement of FSW in manufacturing and automation.

References

1. Thomas W et al (1995) Friction stir butt welding, U.S. Patent 5,460,317, October 24
2. Schneider J (2007) Temperature distribution and resulting metal flow, friction stir welding and processing, ASM International, Chapter 3, pp 37–50
3. Smith C (2000) Robotic friction stir welding using a standard industrial robot. 2nd Friction Stir Welding International Symposium. Gothenburg, Sweden
4. Soron M, Kalaykov I (2006) A robot prototype for friction stir welding, robotics, automation and mechatronics, 2006 IEEE Conference, pp 1–5
5. Zhao X, Kalya P, Landers R, Krishnamurthy K (2007) Design and implementation of a nonlinear axial force controller for friction stir welding processes. proceedings of the 2007 American Control Conference, pp 5553–5558
6. Craig John (2005) Introduction to robotics mechanics and control, 3rd edn. Pearson Prentice Hall
7. Fleming P (2009) Monitoring and control in friction stir welding, PhD Dissertation, Vanderbilt University
8. Ogata (2002) Linear control theory, 4th edn. Pearson Prentice Hall
9. Nunes A, Bernstein E, McClure J (2000) A rotating plug model for fiction stir welding, Presented at 81st American Welding Society Annual Convention
10. Wikipedia, http://en.wikipedia.org/wiki/Friction_stir_welding, 2009